GALLOPING OSCILLATIONS OF PRISMS AND ENERGY HARVESTING IN WIND TUNNEL

P. Hémon[+1], X. Amandolese[+2] and T. Andrianne[+3]
[+1]LadHyX, Ecole Polytechnique-CNRS, Palaiseau, France
[+2]LadHyX, Ecole Polytechnique-CNRS, Palaiseau, and CNAM, Paris, France
[+3]Aerospace and Mechanical Engineering Department, University of Liège, Belgium

We consider the galloping oscillations of prisms with square and 2/3 rectangular section. Rigid prisms are flexibly mounted in wind tunnel. Energy harvest is performed by a series of magnets mounted on the oscillating prism so that they pass close to the face of a coil-core system externally fixed. The produced power is dissipated through a decade box allowing adjustment of the load resistance. A simple mechanical analysis leads to define several efficiencies for such a galloping setup: the global efficiency is the ratio between electric power and wind power. It is the product of two efficiencies: the ratio of the galloping power referred to wind power, and the one being the electrical power referred to the galloping power. Galloping power is the maximum power that can be extracted from the oscillations of the prism which are governed by the aerodynamic damping and structural damping. It is always found very small compared to wind power. Experimental results notably show that there exists an optimal load resistance for global efficiency while another optimal value is found for the electrical production referred to the galloping power.

Keyword: galloping, energy harvest, wind tunnel

1. INTRODUCTION

We consider the galloping oscillations of prisms with square and 2/3 rectangular section shown Fig. 1. Galloping is a dynamic instability that can affect a slender structure submitted to a cross flow. It is a one degree of freedom instability, in transverse or torsional motion, for which the motion-induced fluid loading creates a negative added damping that trigs the instability beyond a critical velocity.

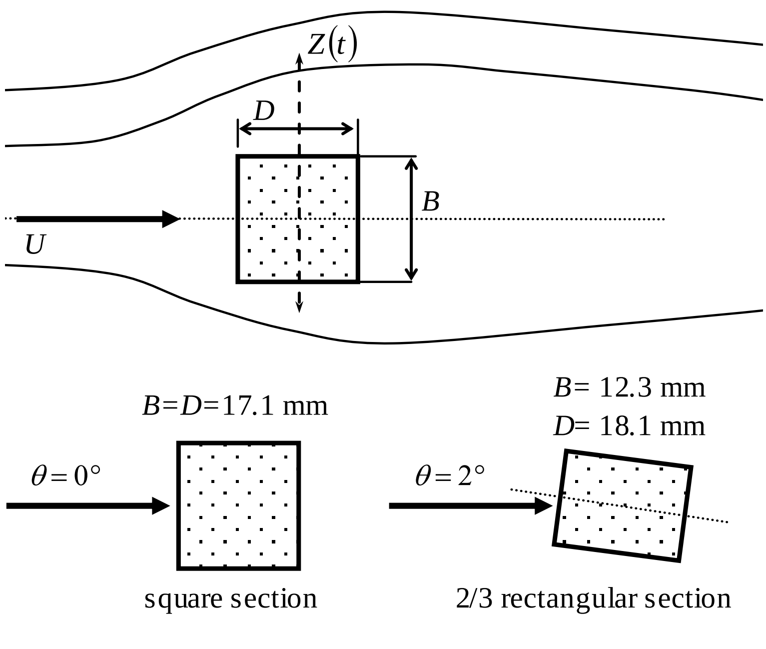

Figure 1: The studied prisms

[+1]hemon@ladhyx.polytechnique.fr, [+2]amandolese@ladhyx.polytechnique.fr, [+3]t.andrianne@ulg.ac.be

Slender structures with non-circular bluff cross section are all susceptible to transverse galloping. The literature on transverse galloping is then important and one can find the most significant references in the book of Blevins [1), the article of Parkinson [2), and the recent book of Païdoussis *et al.* [3). The basic mechanism of transverse galloping along with a quasi-static criterion for the onset of instability was first proposed by Den Hartog in 1934 [4), in the context of transmission line vibration due to sleet.

Once the system is unstable, oscillations growth in amplitude up to limit-cycle regime due to structural or aerodynamic nonlinearities. If one wants to study the post-critical behavior it is then necessary to take into account the nonlinear evolution of the transverse fluid force. This was early done by Parkinson and Brooks [5), Parkinson and Smith [6) and Novak [7) using a nonlinear quasi-steady approach.

Later a number of studies were done on the nonlinear galloping behavior. Effect of turbulence on galloping can also be found in Novak and Tanaka [8). The hysteresis behavior in post-critical galloping is also a matter of concern. Following the work of Parkinson and Smith [6), Luo et al. [9) performed a numerical study focusing on the hysteresis oscillation for the case of a square prism. The link between inflexion points and LCOs hysteresis response was also recently scrutinized by Barrero-Gil et al. [10). In another study, Andrianne and Dimitriadis [11) showed that a fifth-order expansion is sufficient to capture the bifurcation behavior of galloping.

In that context, the objective of this paper is to evaluate and discuss the energy harvesting potential of the galloping mechanism. Energy harvesting from transverse galloping has been previously studied analytically by Barrero-Gil et al. [12) and Vicente-Ludlam et al. [13). This paper is an experimental contribution that could allow to improve the mathematical models and to assess the performances on an engineering point of view.

2. EXPERIMENTAL SETUP

Tests have been performed in an Eiffel open-loop wind tunnel with a square closed test section of 180 by 180 mm. The air inlet is equipped with honeycomb and thin grid so that the turbulence intensity is less than 1% in the test section. The mean velocity can be varied from 5 to 25 m/s by means of a centrifugal fan. The reference velocity is measured via a Pitot tube and a Furness pressure transmitter. Air density is corrected by measurement of the air temperature in the wind tunnel with a thermocouple and the atmospheric pressure with a mercury barometer. Global accuracy of the reference velocity measurement is considered better than 1 %. Data acquisition is performed using a PAK system furnished by Muller-BBM. It is based on a 8 channels analyzer with 24 bits of resolution and sampling frequencies up to 52 kHz.

Two prisms have been used in the study. The first one has a square section and the second one has a rectangular section of ratio B/D = 2/3 shown Fig. 1. Both are made of aluminum alloy with a span 170 mm. Their shape has been adjusted on a milling machine in order to produce corners with sharp edge. In what follows, the reference length is chosen to be D. For the case of the rectangular section it corresponds to the long dimension. The prism models that almost span the test section are equipped with two end plates to keep the airflow as two-dimensional as possible. They are elastically supported in order to allow a one-degree-of-freedom transverse motion $Z(t)$. Stiffness is provided by combination of linear and laminated springs, suitably mounted in order to produce a very low structural damping. These springs are mounted outside the test section, via two vertical fences (see Fig. 2). Length of laminated springs is large (0.75 m) compared to the expected cylinder vertical displacement so that the system can be considered as linear in the range of use.

The vertical displacement of the cylinder is measured by a laser sensor, i.e. without contact that could corrupt damping of the system. It is connected to the acquisition system providing time histories of the signal and simultaneous spectral analysis. Typically a record is 45 s long and the frequency resolution is 1/8 Hz.

Structural parameters of the system were identified under zero-wind velocity. A static weight calibration technique was used to measure the stiffness of the setup. Free decay tests were then performed to identify the natural frequency, by spectral analysis, and the damping ratio using a standard decrement technique. The total mass of the system was then calculated using the measured stiffness and natural frequency. Results are reported in Table 1.

Table 1. Structural characteristics of the two prisms

	Square	Rectangular
frequency (Hz)	5.875	5.75
mass (kg)	0.340	0.326
reduced damping (%)	0.188 ± 0.007	0.256 ± 0.009
stiffness (N/m)	467.1	425.5
Scruton number S_c	21.5	24.9

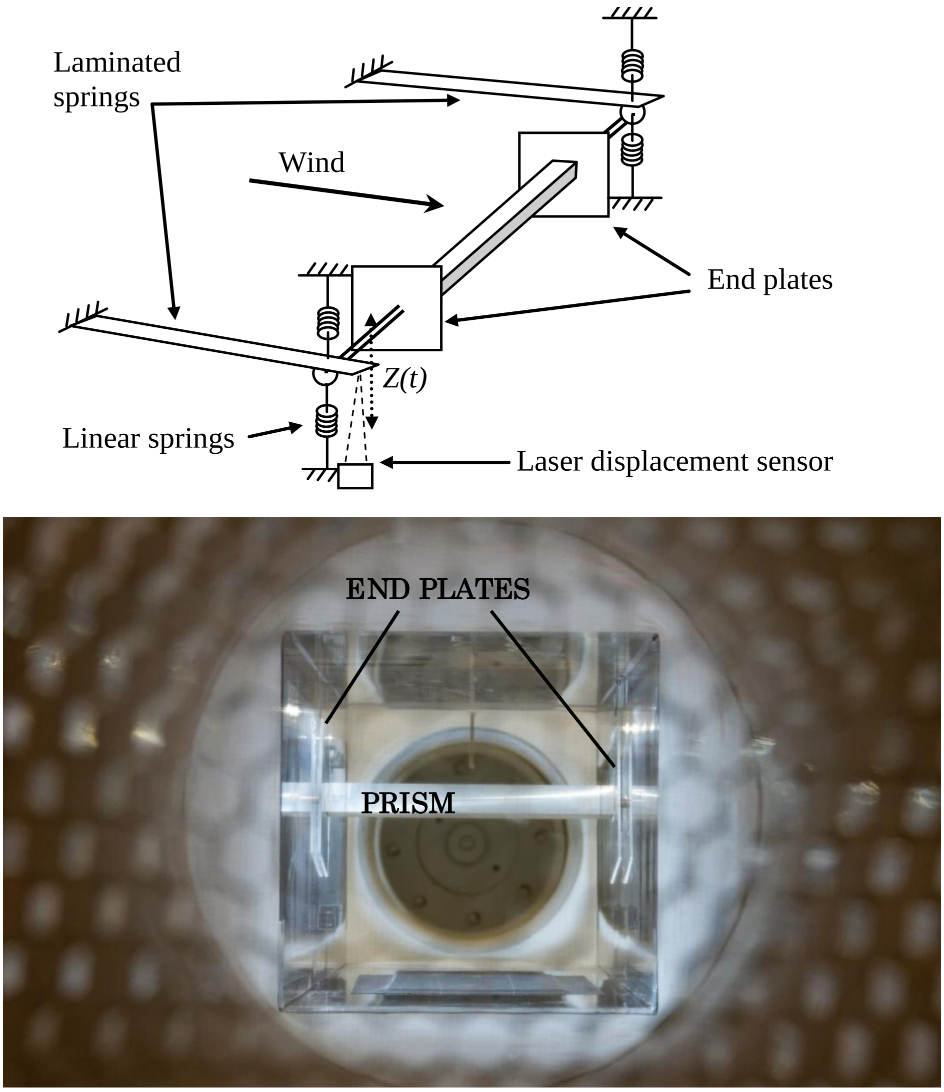

Figure 2. Principle of the experimental setup for galloping and picture taken through the inlet of the wind tunnel

The harvesting device consists in the combination of magnets in motion in the close vicinity of a coil and core static ensemble. The system is depicted in Fig. 3, where the variable electric load is represented. The magnets are located on the suspension beams that ensure the vertical stiffness of the aeroelastic system.

The magnet combination is composed of three Neodymium magnets (NdFeB) of size 10x5x3 mm, with a magnetization type N45. Attraction force of one magnet is 1.5 kg (furnisher data). The total mass of the magnets is equal to 3.33 g. The dimensions of the coil are 22 mm long and 16 mm diameter. Measured inductance is 0.0372 Henry and its electric resistance is 37 Ω. The cylindrical core is 17 mm long and 6 mm diameter. The distance between magnets and coil is 0.5 mm, which places the core at 5.5 mm from the magnets. The load resistance of the harvesting device is adjustable between 0 Ω (short-circuit) up to 10 MΩ (open-circuit). A decade box from Time Electronics is used in the set-up. The load voltage *Vc(t)* is measured synchronously with the vertical displacement *Z(t)* using the PAK system.

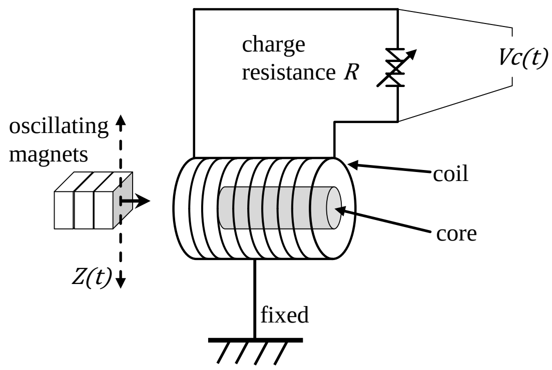

Figure 3. Principle of the electric energy harvesting device

The harvesting device is characterized through shaker tests. A sinusoidal motion of constant amplitude (Z_{rms} = 7.2mm) and frequency (5.75 Hz, see Table 1) is imposed to the magnets in front of the coil. The RMS voltage is measured for different values of the load resistance between 1 Ω and 9 MΩ. Figure 4 shows that the maximum power is reached at 35 Ω. This value is close from the resistance of the coil (37 Ω), in accordance with the Maximum Power Transfer Theorem.

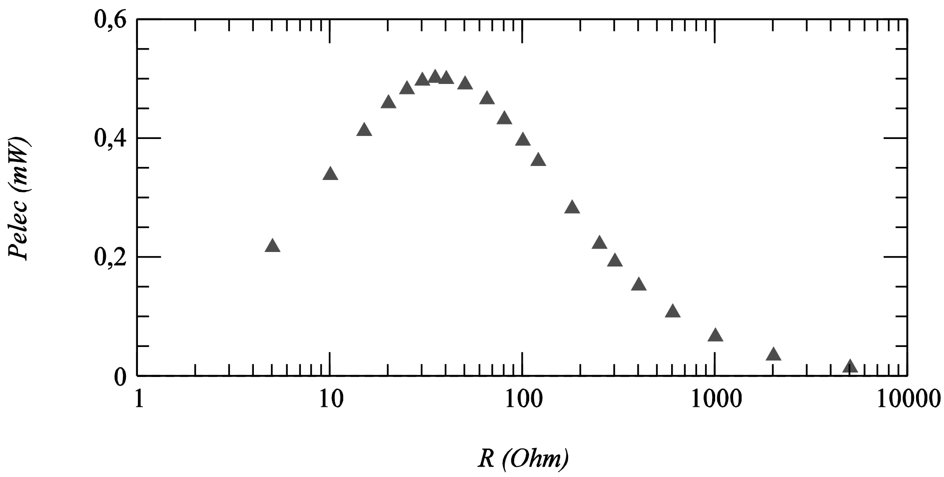

Figure 4. Optimal load resistance of the harvesting device

3. GALLOPING OSCILLATION AMPLITUDE

The aeroelastic response of the square prism is shown Fig. 5 and Fig. 6 for the rectangular prism. The two configurations, i.e. the square prism at θ=0° and the rectangular prism at θ=2°, have been chosen from the results of a previous study showing their good potential, Hémon et al.[14)]. In both cases, the response without energy harvest was measured, with and without the core, since it could affect the response amplitude. Results show that with the chosen settings for the harvesting setup, this is not the case.

The square prism presents a quasi linear growth of amplitude with reduced velocity. When harvesting device is active with its optimal setting (R=90 Ω, see section 5) the response amplitude is lower due to the energy harvest.

But the response of the rectangular prism is slightly different. The linear growth of amplitude occurs beyond Ur=80 after a rapid increase. This is certainly due to the transverse force evolution which is strongly nonlinear for this rectangular prism. When harvesting is active the response is lower and smoothed.

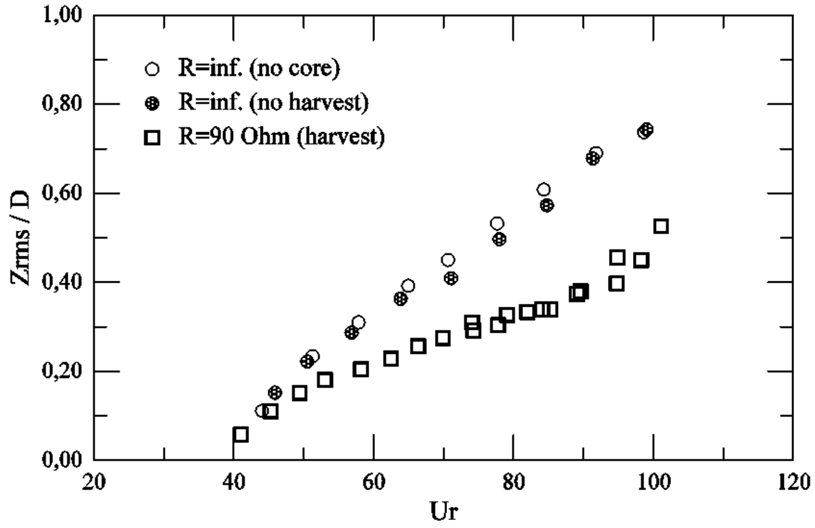

Figure 5: Oscillations amplitude versus reduced velocity for the square prism at θ=0°

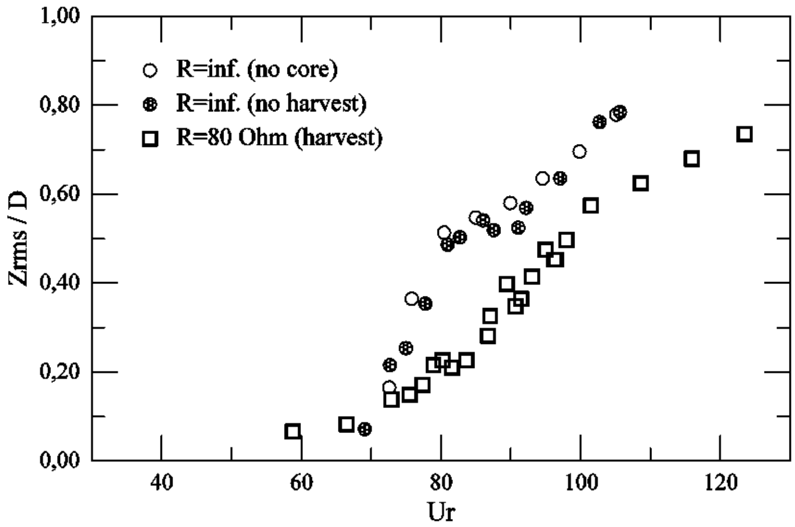

Figure 6: Oscillations amplitude versus reduced velocity for the 2/3 rectangular prism at θ=2°

4. EFFICIENCIES AS A FUNCTION OF REDUCED VELOCITY

The efficiency of energy harvesting is based on the harvested power, i.e. the electric power P_e and the available power in the wind flow P_w. Electric power is defined as:

$$P_e = Vc^2/R \quad (1)$$

where *Vc* is the RMS value of *Vc(t)*. The wind power is defined as the kinetic energy flux of air passing throw a cross section defined as the area swept by the oscillating prism, which is the product of its span and thickness, increased by the measured amplitude oscillations:

$$P_w = \frac{1}{2}\rho\, E\,(D + 2\, Z_{rms})U^3 \quad (2)$$

Another efficiency definition may be of interest for the physical interpretations. Indeed, galloping oscillations are due to the aerodynamic damping and energy harvesting can be performed only from this mechanism. Starting from the linearized equation of motion a characteristic value of the power that can be harvested is defined as:

$$P_g = \frac{1}{T}\int_0^T \left(-\frac{1}{2}\rho DEUCz' - 2\,Em\omega\eta\right)\dot{Z}^2\,dt \qquad (3)$$

where the transverse lift force derivative Cz' is deduced from the critical velocity measured during the free galloping tests. Assuming a periodic motion such as $Z(t) = \sqrt{2}Z_{RMS}\ sin\omega t$ we can compute analytically the previous expression so that:

$$P_g = \left(-\frac{1}{2}\rho DUCz' - 2\,m\omega\eta\right)E\omega^2\,Z_{RMS}^2 \qquad (4)$$

Then the global efficiency can be expressed as the product of two components, an efficiency of the galloping behaviour times the efficiency of the mechanical-electrical process:

$$\frac{P_e}{P_w} = \frac{P_g}{P_w}\frac{P_e}{P_g} \qquad (5)$$

The first ratio in (5) is interesting in the sense that it is independent from the electrical production system and should then be the first quantity to analyze in order to choose the best configuration of prism galloping.

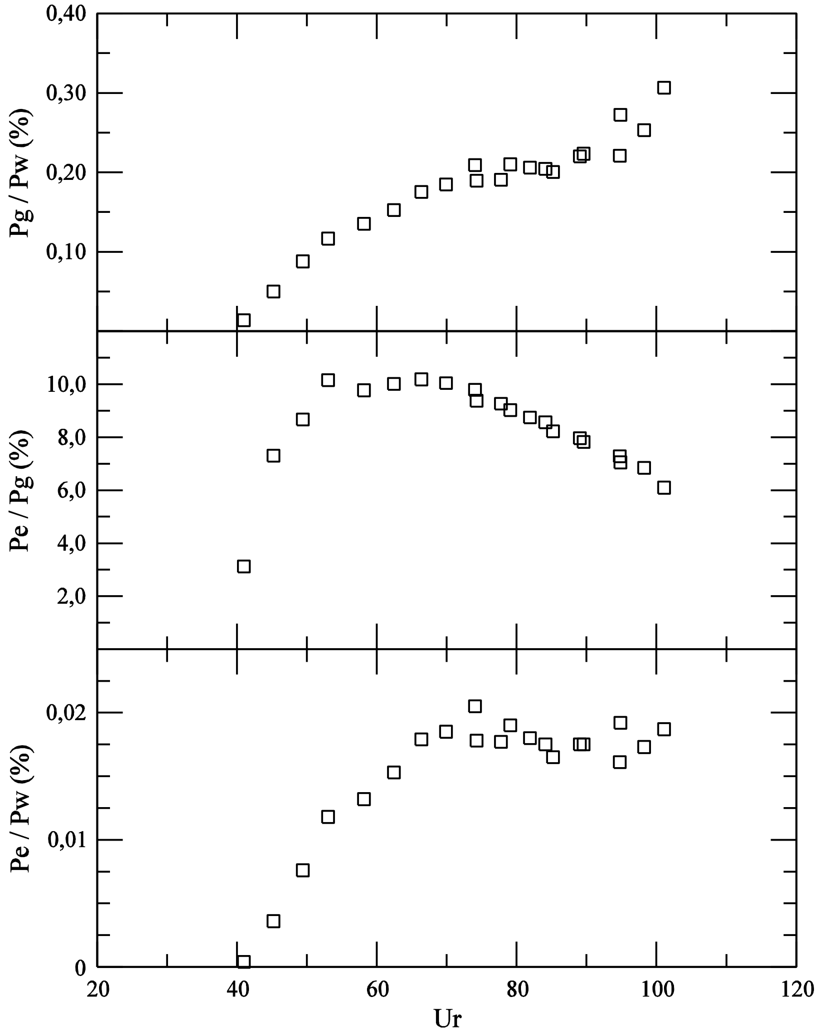

Figure 7: Effiencies of the energy harvest versus reduced velocity for the square prism at θ=0° and optimal load resistance R=90 Ω

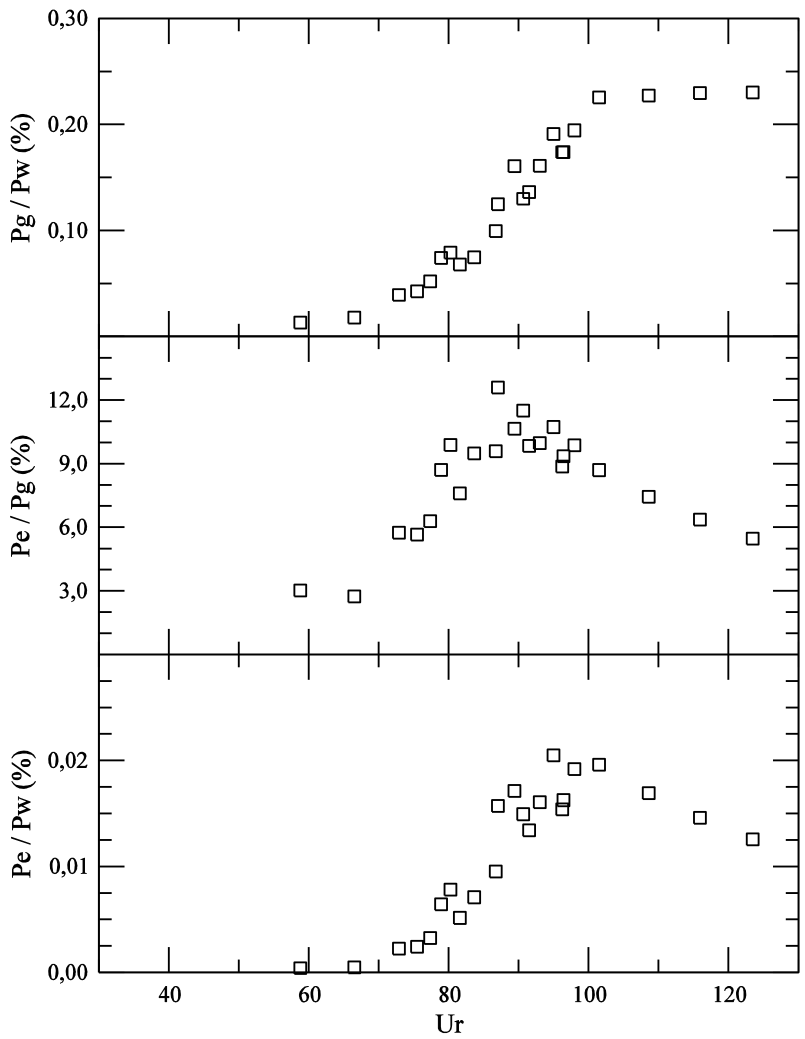

Figure 8: Effiencies of the energy harvest versus reduced velocity for the 2/3 rectangular prism at θ=2° and optimal load resistance R=80 Ω

These three efficiencies are given in Fig. 7 for the square prism and Fig. 8 for the rectangular prism. The main observation is the very low value of the galloping power compared to the wind power, around 0.2-0.3 %. On the other hand, the energy converter, although its simplicity, reaches efficiencies that rise over 10 % in the best conditions.

Finally the global efficiency, which is the product of the two previously mentioned efficiencies, is therefore very small, around 0.02 %. However, to the authors knowledge, the experimental investigation of the potential energy harvesting from galloping oscillations was not published before. On an engineering point of view the extreme simplicity and scalability of the vibrating beam under galloping is an important advantage on the classical horizontal axis wind turbine. It is also very noiseless which is certainly an additional advantage in the context of urban area.

5. THE EFFECT OF THE LOAD RESISTANCE

In order to complete the study, the effect of the load resistance is investigated. Experiments are carried out at constant velocity and the resistance is varied through the decade box. Results are reported in Fig. 9 for the square prism and Fig. 10 for the rectangular prism. At high value of resistance, energy harvest is negligible and the oscillations amplitude match those previously measured (Fig. 5 & 6). As far as the resistance decreases, the oscillations amplitude decreases also and the galloping power decreases more rapidly (proportional to Z_{RMS}^2) than wind power (proportional to Z_{RMS}). Concerning electric power related to galloping power, the resulting efficiency is similar to the energy converter characteristics (Fig. 4) with an optimal resistance close to 40 Ω.

Finally, the global efficiency measuring the ratio between electric power and wind power presents an optimal load resistance which differs from the one mentioned above. It is found around 90 Ω for the square prism and 80 Ω for the rectangular prism, mostly the same value, and independent of the reduced velocity (in the range of tests).

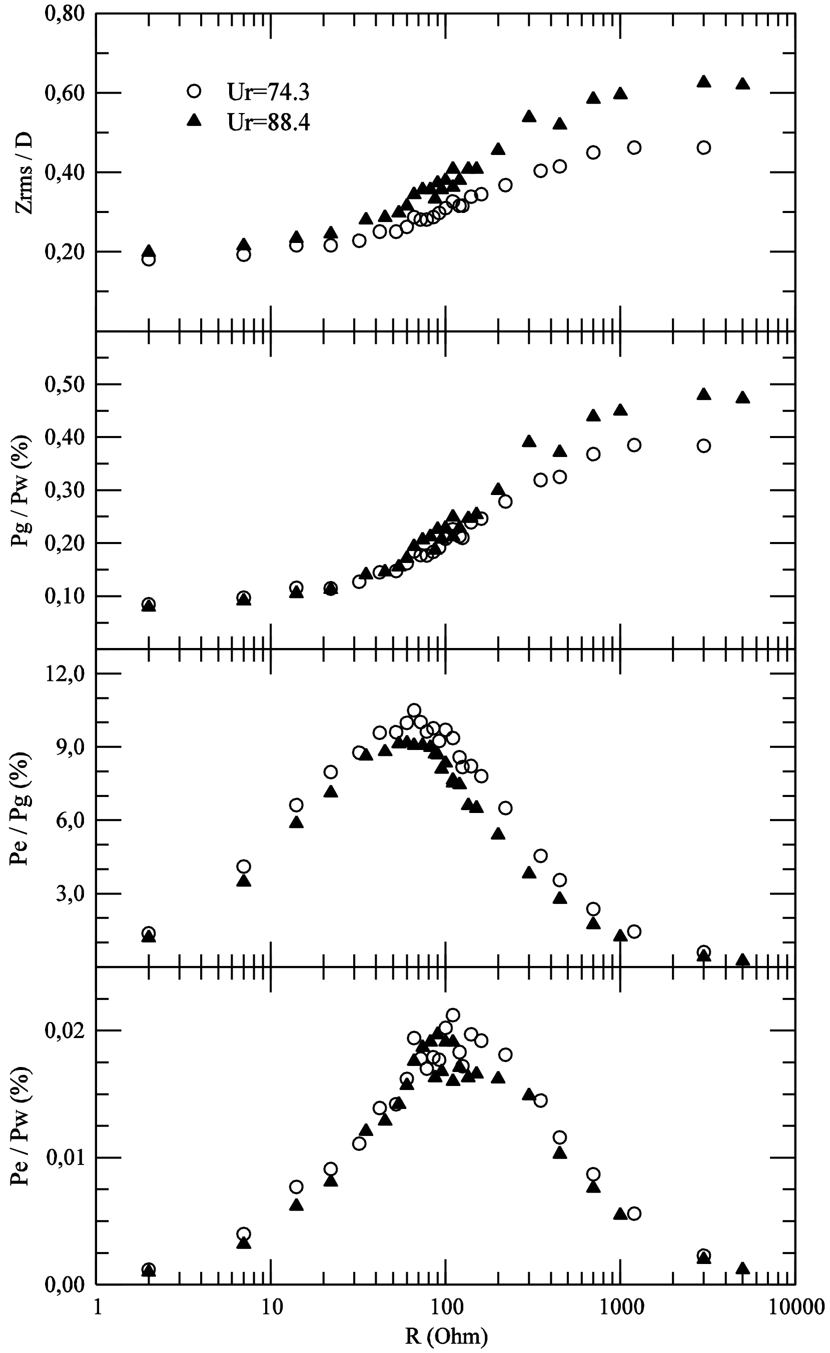

Figure 9: Oscillations amplitude and energy harvest efficiencies versus the electric load resistance for the square prism at θ=0°

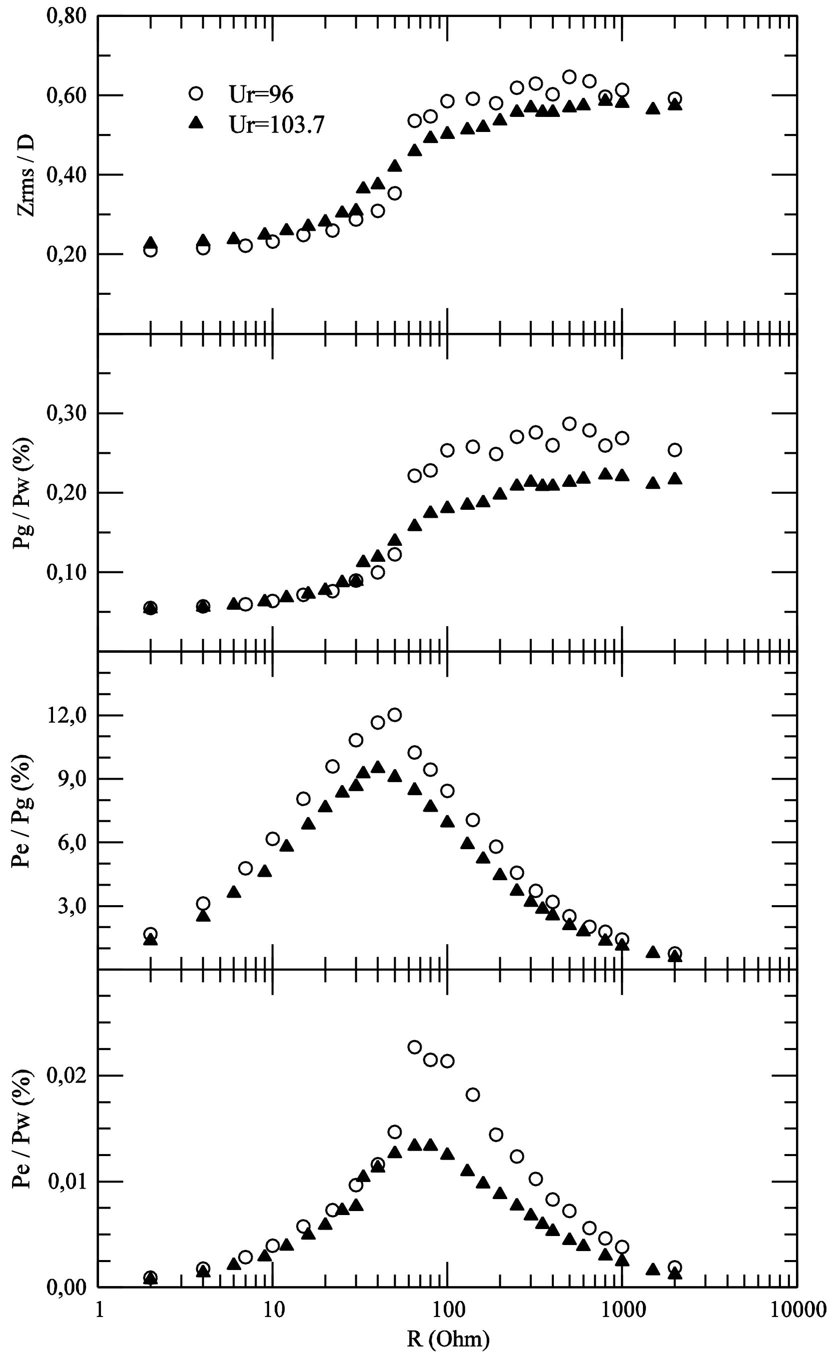

Figure 10: Oscillations amplitude and energy harvest efficiencies versus the electric load resistance for the 2/3 rectangular prism at θ=2°

6. CONCLUSION

Galloping of prisms was investigated experimentally in wind tunnel in order to estimate the potential of this mechanism for producing electric power from the wind. Two configurations were chosen, a square section prism and a 2/3 section prism slightly inclined from the wind direction. A very simple energy harvester system is mounted. It consists in magnets located on the moving prism in front of a coil-core at rest. Efficiency of the system is found very small compared to standard wind turbine due to the galloping mechanism physics. However the electromechanical setup converting translating motion in electric energy is interesting and could certainly improved.

Experiments show also that there exist two optimal load resistances, one linked to the galloping mechanism and another one linked to the energy converter. Next step of this study could be the design of another setup in which these optimal resistance are joined, which probably could lead to the best efficiency of such a system.

Although efficiency of this "prism wind turbine" is rather weak, it remains interesting to further investigations and optimization because of its extreme simplicity and cost. Moreover such kind of system can be developed at various scales, for water current or wind and, because of the noiseless functioning, it can be placed in a number of situations where standard wind turbines cannot.

REFERENCES

1) Blevins, R. D. Flow-Induced Vibrations. Reprint of the 1990 second edition, Krieger Publishing Company, Malabar, Florida. 2001.

2) Parkinson, G. V. Phenomena and modelling of flow-induced vibrations of bluff bodies. *Progress in Aerospace Sciences 26(2)*, pp. 169-224. 1989.

3) Païdoussis, M. P., Price, S. J., De Langre, E. Fluid-structure interactions: cross-flow induced instabilities. Cambridge University Press. 2011.

4) Den Hartog, J.P. Mechanical Vibrations. Reprint of the 1934 edition. Dover, New York. 1985.

5) Parkinson, G. V., Brooks, N. P. H. On the aeroelastic instability of bluff cylinders. ASME *Journal of Applied Mechanics,* June 1961, pp. 252-258. 1961.

6) Parkinson, G. V., Smith, J. D. The Square Prim as an Aeroelastic Non-linear Oscillator. *Quarterly Journal of Mechanics and Applied Mathematics*, XVII, pp. 225-239. 1964.

7) Novak, M. Aeroelastic galloping of prismatic bodies. *J. of the Engineering Mechanics Division of the ASCE*, 96, pp. 115-142. 1969.

8) Novak, M., Tanaka H. Effect of turbulence on galloping instability. *J. of the Engineering Mechanics Division of the ASCE*, 100, pp. 27-47. 1974.

9) Luo, S.C., Chew, Y.T., Ng, Y.T. Hysteresis phenomenon in the galloping oscillation of a square cylinder. *J. Fluids and Structures* 18, pp. 103-118. 2003.

10) Barrero-Gil, A., Sanz-Andrés, A. Alonso, G. Hysteresis in transverse galloping: the role of inflection points. *J. Fluids and Structures* 20, pp. 1007-1020. 2009.

11) Andrianne , T., Dimitriadis, G. Empirical modelling of the bifurcation behaviour of a bridge deck undergoing across-wind galloping, *J. Wind Engineering and Industrial Aerodynamics* 135, pp. 129–135, 2014.

12) Barrero-Gil, A., Alonso, G., Sanz-Andres, A. Energy harvesting from transverse galloping. *J. Sound and Vibration* 329, pp. 2873-2883. 2010.

13) Vicente-Ludlam, D., Barrero-Gil, A., Velazquez, A. Optimal electromagnetic energy extraction from transverse galloping. *J. Fluids and Structures* 51, pp. 281-291. 2014.

14) Hémon, P., Amandolese, X. & Andrianne, T. Galloping oscillations of prisms and energy harvesting in wind tunnel. Submitted to . *J. Fluids and Structures* 2016.